

Applying non-negative matrix factorization with covariates to structural equation modeling for blind input–output analysis

Kenichi Satoh¹

¹Faculty of Data Science, Shiga University, Banba 1-1-1, Hikone, 522-8522, Shiga, Japan.

Contributing authors: kenichi-satoh@biwako.shiga-u.ac.jp;

Abstract

Structural equation modeling (SEM) describes directed dependence and feedback, whereas non-negative matrix factorization (NMF) provides interpretable, parts-based representations for non-negative data. We propose NMF-SEM, a unified non-negative framework that embeds NMF within a simultaneous-equation structure, enabling latent feedback loops and a reduced-form input–output mapping when intermediate flows are unobserved. The mapping separates direct effects from cumulative propagation effects and summarizes reinforcement using an amplification ratio.

We develop regularized multiplicative-update estimation with orthogonality and sparsity penalties, and introduce structural evaluation metrics for input–output fidelity, second-moment (covariance-like) agreement, and feedback strength. Applications show that NMF-SEM recovers the classical three-factor structure in the Holzinger–Swineford data, identifies climate- and pollutant-driven mortality pathways with negligible feedback in the Los Angeles system, and separates deprivation, general morbidity, and deaths-of-despair components with weak feedback in Mississippi health outcomes.

Keywords: Non-negative matrix factorization (NMF), Structural equation modeling (SEM), NMF-SEM, Non-negative structural systems, Blind input–output analysis, Feedback amplification

1 Introduction

Non-negative matrix factorization (NMF) provides an interpretable, parts-based representation of high-dimensional non-negative data (Lee and Seung, 1999, 2000; Cichocki et al, 2009; Gillis, 2014). By decomposing data into additive non-negative components, NMF yields latent factors that are often directly interpretable as meaningful “parts.” Structural equation modeling (SEM), in contrast, specifies directed dependence relations among observed and latent variables and plays a central role in the social sciences, psychology, and econometrics (Zhang et al, 2016). SEM emphasizes structural relations, equilibrium behavior, and the distinction between endogenous and exogenous variables.

Although both frameworks rely on latent structure, they have evolved largely independently: NMF focuses on additive non-negative representations without explicit structural interpretation, whereas SEM focuses on structural relations but typically lacks a parts-based non-negative formulation.

Recent developments in non-negative structural systems (Lodhia et al, 2023; Zhou et al, 2022) demonstrate that imposing non-negativity can enhance the interpretability and stability of SEM-like models. However, these approaches remain covariance- or DAG-based and do not integrate latent factor models with non-negative simultaneous equation systems or equilibrium input–output (IO) analysis. Likewise, NMF-with-covariates ($X\Theta A$) models (Satoh, 2024, 2025b,a) extend NMF in a predictive, regression-oriented direction by incorporating exogenous information, but they are strictly feed-forward and therefore cannot represent the simultaneous latent feedback that underlies SEM and classical IO systems.

Self-expressive models and their integration with non-negative matrix factorization (Galeano and Paccanaro, 2022; Galeano et al, 2024) reconstruct observations using relationships among data points (e.g., $X \approx MX$), encoding local or global similarity structure directly in the data space. Although these models capture relational structure effectively, they do not explicitly specify latent variables, exogenous drivers, or equilibrium behavior. Finally, the classical Leontief input–output model (Leontief, 1936) captures cumulative effects through a non-negative simultaneous equation system, but it assumes that internal flows are fully observed; when such flows are missing, one faces a *blind input–output* problem.

While existing approaches address subsets of these components, none integrates a non-negative latent-factor representation, a cycle-permissive structural system, and an equilibrium IO mapping within a single framework suitable for blind input–output analysis.

This work introduces NMF-SEM, a unified framework bridging NMF, SEM, and IO analysis. We impose a non-negative simultaneous equation system on the NMF coefficient matrix,

$$B = \Theta_1 Y_1 + \Theta_2 Y_2,$$

so that $Y_1 \approx XB$ arises from a latent structural system with endogenous feedback. This construction yields an equilibrium representation, a latent Leontief-type cumulative-effect operator, and a principled decomposition of direct and higher-order feedback effects (Section 2).

Whereas conventional SEM requires the researcher to pre-specify both the latent structure and the pattern of directed paths in order to obtain an identified model, NMF-SEM learns both components automatically under non-negativity. This reduces parametric flexibility compared with general SEM, but yields identifiable, interpretable, and stable equilibrium mappings without pre-specifying a structural graph.

The main contributions are as follows.

- (1) A non-negative simultaneous equation system embedded within NMF, enabling latent feedback and equilibrium behavior.
- (2) An equilibrium input–output mapping whose Neumann expansion separates direct and cumulative effects.
- (3) A formulation of blind input–output analysis in latent space that recovers equilibrium propagation from exogenous to endogenous variables even when internal flows are unobserved.
- (4) A regularized estimation and evaluation framework combining orthogonality, sparsity, and equilibrium-based structural metrics.

Section 3 introduces the regularized multiplicative-update algorithm for estimating (X, Θ_1, Θ_2) , and Section 4 presents equilibrium-based structural metrics. Section 5 demonstrates NMF-SEM across cognitive, environmental, and population-health applications, and Section 6 concludes.

2 The NMF-SEM Model

This section develops the non-negative structural equation model NMF-SEM. The goal is to enrich the parts-based representation of NMF by imposing a non-negative simultaneous equation system on the coefficient matrix. This structural layer induces interpretable direct and feedback effects, and yields an equilibrium mapping analogous to classical input–output (IO) analysis.

2.1 Basic formulation

Let $Y_1 \in \mathbb{R}_+^{P_1 \times N}$ denote endogenous variables and $Y_2 \in \mathbb{R}_+^{P_2 \times N}$ exogenous variables. NMF approximates Y_1 by

$$Y_1 \approx XB, \quad X \in \mathbb{R}_+^{P_1 \times Q}, \quad B \in \mathbb{R}_+^{Q \times N},$$

where the columns of X form latent profiles and the columns of B represent non-negative mixture weights. We normalize each column of X to sum to one so that latent profiles are directly comparable and mixture weights represent shares.

Classical NMF treats B as unconstrained. NMF-SEM instead specifies B through a structural system.

2.2 Structural equation component

We model the coefficient matrix B as a non-negative simultaneous equation system:

$$B = \Theta_1 Y_1 + \Theta_2 Y_2, \quad \Theta_1 \in \mathbb{R}_+^{Q \times P_1}, \quad \Theta_2 \in \mathbb{R}_+^{Q \times P_2}.$$

Here, Θ_1 governs how endogenous variables activate the latent components (feedback), and Θ_2 governs how exogenous drivers activate latent components.

Substituting this expression for B into $Y_1 \approx XB$ gives the structural form of NMF-SEM:

$$Y_1 \approx X(\Theta_1 Y_1 + \Theta_2 Y_2). \quad (1)$$

The composite matrices $X\Theta_1$ and $X\Theta_2$ encode, respectively, direct endogenous interactions and direct exogenous influences in the observed space.

The special case $\Theta_1 = 0$ reduces to the feed-forward $X\Theta A$ family. Allowing $\Theta_1 \neq 0$ introduces latent feedback and leads to an equilibrium representation.

2.3 Equilibrium representation

Rearranging (1) yields

$$(I - X\Theta_1) Y_1 \approx X\Theta_2 Y_2.$$

To ensure that the system converges, we impose the stability condition

$$\rho(X\Theta_1) < 1, \quad (2)$$

where $\rho(\cdot)$ denotes the spectral radius. Under this condition, $(I - X\Theta_1)$ is invertible, and the structural system admits the reduced-form equilibrium mapping

$$Y_1 \approx (I - X\Theta_1)^{-1} X\Theta_2 Y_2. \quad (3)$$

Define the cumulative-effect operator

$$M_{\text{model}} = (I - X\Theta_1)^{-1} X\Theta_2 \in \mathbb{R}_+^{P_1 \times P_2}. \quad (4)$$

This operator combines both direct effects and all rounds of latent feedback. In estimation, we enforce (2) and select hyperparameters only among stable solutions.

2.4 Latent Leontief inverse and cumulative feedback

Because $X\Theta_1$ is non-negative and satisfies (2), the inverse in (3) admits the Neumann expansion

$$(I - X\Theta_1)^{-1} = I + (X\Theta_1) + (X\Theta_1)^2 + \dots. \quad (5)$$

This is the latent analogue of the Leontief inverse in IO analysis. Substituting (5) into (4) shows that

$$M_{\text{model}} = X\Theta_2 + X\Theta_1 X\Theta_2 + (X\Theta_1)^2 X\Theta_2 + \dots,$$

where each term corresponds to additional rounds of latent propagation. All effects accumulate monotonically due to non-negativity.

A useful scalar summary of total amplification due to latent feedback is the amplification ratio:

$$\text{AR} = \frac{\|M_{\text{model}}\|_{1,\text{op}}}{\|X\Theta_2\|_{1,\text{op}}}, \quad (6)$$

where $\|\cdot\|_{1,\text{op}}$ is the operator 1-norm. Values above one indicate amplification generated by latent feedback.

2.5 Amplification bounds

Because $X\Theta_1$ is non-negative, the equilibrium operator $(I - X\Theta_1)^{-1}$ admits the Neumann expansion of non-negative powers of $X\Theta_1$ whenever $\rho(X\Theta_1) < 1$. Consequently,

$$M_{\text{model}} = (I - X\Theta_1)^{-1}X\Theta_2 \geq X\Theta_2, \quad \text{AR} \geq 1,$$

with equality if and only if $X\Theta_1 = 0$.

If $\|X\Theta_1\|_{1,\text{op}} < 1$, submultiplicativity yields

$$\|(I - X\Theta_1)^{-1}\|_{1,\text{op}} \leq \frac{1}{1 - \|X\Theta_1\|_{1,\text{op}}},$$

and therefore the amplification ratio satisfies the two-sided bound

$$1 \leq \text{AR} \leq \frac{1}{1 - \|X\Theta_1\|_{1,\text{op}}}.$$

Thus AR remains finite under the stability condition and increases monotonically with the strength of latent feedback.

2.6 Interpretation of latent structure

The matrix X provides a parts-based representation of Y_1 , grouping variables with similar response profiles into latent components. The matrices Θ_1 and Θ_2 determine how these components are activated: Θ_2 allocates exogenous drivers to latent factors, and Θ_1 induces propagation through latent feedback. The equilibrium operator M_{model} summarizes how shocks to Y_2 translate into equilibrium outcomes in Y_1 .

Non-negativity ensures additive interpretation: increases in Y_2 can only increase (or leave unchanged) the equilibrium values in Y_1 , and feedback effects accumulate rather than offset.

3 Estimation

This section outlines a practical estimation procedure for NMF-SEM. Because the coefficient matrix is constrained by

$$B = \Theta_1 Y_1 + \Theta_2 Y_2,$$

the parameters (X, Θ_1, Θ_2) must be estimated jointly under non-negativity and the equilibrium structure introduced in Section 2. Our approach consists of: (i) initialization via a feed-forward model, (ii) structural regularization, (iii) multiplicative updates, and (iv) hyperparameter selection based on equilibrium prediction error.

3.1 Initialization

When $\Theta_1 = 0$, the structural equation component vanishes and the model reduces to the feed-forward tri-factorization

$$Y_1 \approx X_0 \Theta_0 Y_2,$$

which corresponds to the NMF-with-covariates $(X\Theta A)$ family (Satoh, 2025b,a). This special case provides a natural starting point for NMF-SEM: the feed-forward solution (X_0, Θ_0) captures the direct effects Θ_2 without latent feedback, and serves as a stable and interpretable initialization for estimating the full system (X, Θ_1, Θ_2) .

We therefore estimate (X_0, Θ_0) using an NMF-with-covariates algorithm and use X_0 as the initial latent basis. The associated mapping

$$M_{\text{simple}} = X_0 \Theta_0$$

is later used as a structural benchmark when assessing IO fidelity in Section 4. Initialization employs either k -means or the NNDSVDar method (Boutsidis and Gallopoulos, 2008), which reduces sensitivity to random starts.

3.2 Structural regularization

To resolve rotational ambiguity and stabilize latent feedback, we employ a penalized objective:

$$L = \|Y_1 - X(\Theta_1 Y_1 + \Theta_2 Y_2)\|_F^2 + \frac{\lambda_X}{2} \|X^\top X - \text{diag}(X^\top X)\|_F^2 + \lambda_1 \|\Theta_1\|_1 + \lambda_2 \|\Theta_2\|_1.$$

The orthogonality penalty encourages separated latent components, while the ℓ_1 penalties promote sparse structural pathways and regularize the feedback matrix $X\Theta_1$.

3.3 Multiplicative updates

Let $B = \Theta_1 Y_1 + \Theta_2 Y_2$ and $\hat{Y}_1 = XB$. Ignoring penalties, standard auxiliary-function arguments yield the following multiplicative updates, which generalize the classical Lee–Seung rules for NMF (Lee and Seung, 1999, 2000):

$$X \leftarrow X \odot \frac{Y_1 B^\top}{X B B^\top}, \quad \Theta_1 \leftarrow \Theta_1 \odot \frac{X^\top Y_1 Y_1^\top}{X^\top \hat{Y}_1 Y_1^\top}, \quad \Theta_2 \leftarrow \Theta_2 \odot \frac{X^\top Y_1 Y_2^\top}{X^\top \hat{Y}_1 Y_2^\top}.$$

Under regularization, the denominators incorporate the corresponding gradients:

$$X \leftarrow X \odot \frac{Y_1 B^\top}{X B B^\top + \lambda_X X (X^\top X - \text{diag}(X^\top X))},$$

$$\Theta_1 \leftarrow \Theta_1 \odot \frac{X^\top Y_1 Y_1^\top}{X^\top \hat{Y}_1 Y_1^\top + \lambda_1}, \quad \Theta_2 \leftarrow \Theta_2 \odot \frac{X^\top Y_1 Y_2^\top}{X^\top \hat{Y}_1 Y_2^\top + \lambda_2}.$$

Columns of X are renormalized after each update. These multiplicative rules decrease L monotonically in practice.

3.4 Hyperparameter selection

Regularization parameters $(\lambda_X, \lambda_1, \lambda_2)$ control orthogonality, sparsity, and feedback magnitude. Because reconstruction error does not reflect the equilibrium structure introduced in Section 2, hyperparameters are selected by cross-validating the equilibrium prediction performance using the mapping $Y_1 \approx M_{\text{model}} Y_2$ defined in (4).

For each held-out fold, equilibrium predictions are computed from the estimated M_{model} , and prediction accuracy is quantified by the mean absolute error (MAE), defined as the average absolute deviation across all entries of Y_1 and \hat{Y}_1 . We fix λ_X at a value enforcing approximate orthogonality (e.g. 100) and choose (λ_1, λ_2) by K -fold cross-validation, subject to the stability requirement $\rho(X\Theta_1) < 1$.

4 Evaluation

NMF-SEM is designed for structural interpretation. Accordingly, evaluation focuses on whether the estimated model (1) preserves key input–output (IO) relationships, (2) reproduces second-moment structure among endogenous variables, (3) captures the strength of latent feedback, and (4) yields a reasonable equilibrium approximation. We summarize the corresponding metrics below.

4.1 Input–output structural fidelity

The equilibrium operator

$$M_{\text{model}} = (I - X\Theta_1)^{-1} X\Theta_2$$

summarizes the total effect of exogenous variables on endogenous ones. To assess whether NMF-SEM preserves the qualitative IO structure implied by the feed-forward initialization, we compare M_{model} with $M_{\text{simple}} = X_0\Theta_0$ using the correlation

$$\text{SC}_{\text{map}} = \text{Cor}(\text{vec}(M_{\text{model}}), \text{vec}(M_{\text{simple}})). \quad (7)$$

High values indicate that the estimated feedback-enhanced mapping remains consistent with the direct-effect structure.

4.2 Second-moment fidelity

Equilibrium predictions $\widehat{Y}_1 = M_{\text{model}}Y_2$ induce a second-moment structure among endogenous variables given by

$$S_{\text{model}} = \widehat{Y}_1 \widehat{Y}_1^\top = M_{\text{model}} S_{Y_2} M_{\text{model}}^\top, \quad S_{Y_2} = Y_2 Y_2^\top.$$

This matrix summarizes the dependence pattern implied by the equilibrium input-output mapping. We compare it with the empirical second-moment matrix $S_{\text{sample}} = Y_1 Y_1^\top$ via

$$\text{SC}_{\text{cov}} = \text{Cor}(\text{vec}(S_{\text{model}}), \text{vec}(S_{\text{sample}})), \quad (8)$$

which evaluates whether the equilibrium mapping reproduces the observed second-moment structure among endogenous variables.

Throughout this paper, second-moment matrices are treated as covariance-like summaries of dependence. All variables are pre-processed to a common scale to facilitate interpretation of structural evaluation metrics, not for estimation itself. As in classical SEM, such scaling is optional for estimation but improves the interpretability of structural comparisons.

4.3 Feedback strength

Latent feedback is summarized by two quantities: the spectral radius $\rho(X\Theta_1)$ and the amplification ratio AR defined in Section 2.4. The former captures the intrinsic strength of the latent feedback loop, while AR compares total equilibrium effects with direct effects. Here, latent feedback should be interpreted as a parsimonious structural representation of residual dependence among endogenous variables not explained by observed exogenous variables, under the assumption that the observed endogenous variables reflect equilibrium outcomes rather than transient dynamics.

Sampling uncertainty for both measures is assessed by a nonparametric bootstrap: we resample the columns of (Y_1, Y_2) with replacement, refit the model under fixed hyperparameters, and compute percentile intervals for $\rho(X\Theta_1)$ and AR.

4.4 Simulation summary

To verify that the proposed metrics behave coherently when the true system is known, we conducted Monte Carlo experiments under controlled data-generating conditions. We varied both the noise level $\sigma \in \{0, 0.05, 0.10\}$ and the strength of latent feedback $\rho_{\text{true}} \in \{0, 0.2\}$ in order to assess the sensitivity of each metric to these key structural features. In each setting, synthetic data were generated from fixed non-negative parameters $(X_{\text{true}}, \Theta_{1,\text{true}}, \Theta_{2,\text{true}})$, and samples of size $N \in \{50, 200\}$ were drawn. Models were then fitted using the estimation procedure described in Section 3, and results were aggregated over $R = 500$ replications.

Table 1 reports the noise-free results ($\sigma = 0$). These provide a baseline for evaluating the behavior of the metrics without sampling noise.

Across all conditions, AR increased with the estimated feedback $\rho(X\Theta_1)$ and with sample size, consistent with the geometric amplification bound in Section 2.5. Larger samples yield more stable estimates of the small positive entries in Θ_1 , producing larger

Table 1 Noise-free simulation results ($\sigma = 0$, $R = 500$). Values are means across replications.

Condition	ρ_{hat}	AR _{hat}	SC _{map}	SC _{cov}	MAE
$\rho_{\text{true}} = 0$, $N = 50$	0.138	1.20	0.995	0.998	0.006
$\rho_{\text{true}} = 0$, $N = 200$	0.434	3.09	0.996	0.998	0.007
$\rho_{\text{true}} = 0.2$, $N = 50$	0.209	1.63	0.994	0.997	0.008
$\rho_{\text{true}} = 0.2$, $N = 200$	0.578	4.70	0.992	0.998	0.010

column sums in $X\Theta_1$ and hence higher amplification through $(I - X\Theta_1)^{-1}$. Overall, the proposed metrics capture the essential behavior of non-negative latent–feedback systems and respond coherently to controlled changes in the data-generating process.

In finite samples, $\rho(X\Theta_1)$ does not shrink exactly to zero even when $\Theta_{1,\text{true}} = 0$, because small positive estimates arise from sampling variation and the non-negativity constraints. This explains the mild positive bias observed in the $\rho_{\text{true}} = 0$ conditions.

5 Applications

Before presenting the empirical studies, we clarify the interpretation of the path diagrams shown in this section. Although visually similar to diagrams in classical structural equation models (SEMs), all arrows in NMF-SEM represent non-negative additive contributions rather than signed regression effects, and the latent feedback structure reflects the equilibrium mechanism introduced in Section 2.3. Thus the diagrams summarize the equilibrium input–output mapping $Y_2 \mapsto Y_1$, not a covariance-based system among latent variables.

With this distinction, we illustrate the practical utility of NMF-SEM through three empirical examples spanning different domains and feedback regimes. Table 2 summarizes the key structural and predictive metrics defined in Section 4, including the latent dimension Q , feedback strength $\rho(X\Theta_1)$, amplification ratio (AR), structural correlations for the input–output and second-moment mappings, and equilibrium MAE. The table also reports bootstrap percentile intervals for $\rho(X\Theta_1)$ and AR, obtained using the procedure described in Section 4.3.

Across the three datasets, the Holzinger–Swineford cognitive tests show moderate latent amplification with near-perfect structural fidelity; the Los Angeles pollution–mortality system exhibits an almost purely feed-forward structure; and the Mississippi health-risk data display weak but non-zero latent feedback. These contrasts highlight the flexibility of NMF-SEM in capturing both direct and cumulative effects across diverse settings.

Bootstrap percentile intervals confirm that the estimates of $\rho(X\Theta_1)$ and AR are stable, and the qualitative conclusions reported below are robust.

The remainder of this section examines each dataset in turn, focusing on the recovered latent components, the estimated exogenous pathways, and the role of feedback in shaping cumulative effects.

Table 2 Structural and predictive metrics for the three empirical datasets. Values in parentheses denote 95% bootstrap percentile intervals based on resampling the (Y_1, Y_2) columns and refitting NMF-SEM with fixed hyperparameters. Sample sizes were $N = 301$ (HS39), $N = 508$ (LA), and $N = 36$ (Mississippi), with latent dimensions $Q = 3, 2$, and 3 , respectively.

Dataset	$\rho(X\Theta_1)$	AR	SC_{map}	SC_{cov}	MAE
Holzinger–Swineford	0.350 (0.23–0.68)	1.358 (1.21–1.51)	0.999	0.980	0.181
Los Angeles pollution–mortality	0.003 (0.00–0.01)	1.002 (1.00–1.01)	0.882	0.983	0.095
Mississippi health risks	0.441 (0.06–0.60)	1.029 (1.00–1.26)	0.935	0.989	0.116

5.1 Holzinger–Swineford cognitive-ability analysis

The first application uses the classical Holzinger–Swineford (HS39) cognitive-test dataset (Holzinger and Swineford, 1939), a standard benchmark in factor analysis (Jöreskog, 1969). Nine test scores were treated as endogenous variables, and three background variables (reversed age, gender, school indicator) were used as exogenous inputs after rescaling all variables to $[0, 1]$. NMF-SEM was fitted with latent dimension $Q = 3$, corresponding to the established three-factor structure.

The estimated basis matrix X (Table 3) recovers the canonical grouping of visual ($x1$ – $x3$), verbal ($x4$ – $x6$), and speeded-performance ($x7$ – $x9$) tests, showing that NMF-SEM extracts the classical ability pattern in a non-negative and data-driven manner.

Table 3 Estimated basis matrix X for the HS39 data ($Q = 3$).

Variable	Factor 1	Factor 2	Factor 3
$x1$ (visual)	0.28	0.01	0.00
$x2$ (cubes)	0.25	0.04	0.00
$x3$ (lozenges)	0.26	0.00	0.00
$x4$ (paragraph)	0.00	0.31	0.00
$x5$ (sentence)	0.00	0.37	0.00
$x6$ (word)	0.00	0.22	0.00
$x7$ (add)	0.00	0.00	0.64
$x8$ (dots)	0.05	0.02	0.28
$x9$ (caps)	0.16	0.02	0.08

The latent-feedback operator $X\Theta_1$ was sparse, with feedback pathways from representative variables to their associated factors (e.g., $x3$ for visual, $x5$ for verbal, $x7$ for speed). Feedback strength was moderate, with spectral radius $\rho(X\Theta_1) \approx 0.35$ and amplification ratio $AR \approx 1.36$.

Exogenous inputs showed expected patterns, with reversed age affecting all factors and school membership primarily influencing the verbal component. Structural fidelity was high: IO structural correlation exceeded 0.99, covariance structural correlation was near 0.98, and the equilibrium MAE was approximately 0.18.

Overall, the HS39 results demonstrate that NMF-SEM recovers the familiar three-factor structure while quantifying modest latent feedback in a non-negative framework.

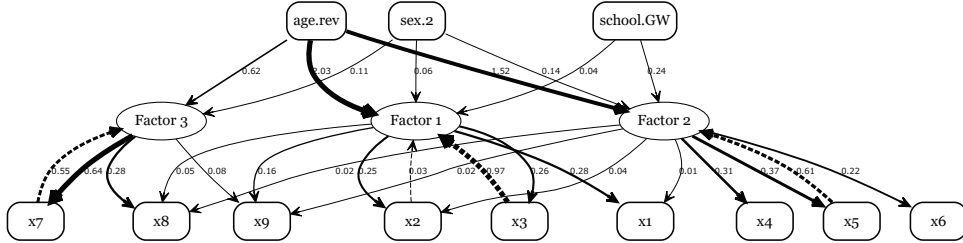


Fig. 1 Path diagram estimated by NMF-SEM ($Q = 3$) for the HS39 dataset, showing the recovered three-factor structure and moderate latent feedback (amplification ratio ≈ 1.36).

5.2 LA pollution–mortality analysis

We analyzed the `lap` dataset from the `astsa` package (Shumway and Stoffer, 2006), which contains weekly mortality counts together with climatic variables and pollutant concentrations (CO, SO₂, NO₂, hydrocarbons, ozone, particulates) from 1970–1979. Endogenous variables (Y_1) consist of total, respiratory, and cardiovascular mortality; exogenous variables (Y_2) include temperature, humidity, pollutant levels, and a quadratic temperature term. Mortality counts were log-transformed and all variables were rescaled to [0, 1] with signs adjusted so that larger values indicate higher risk.

Cross-validation selected a latent dimension of $Q = 2$. NMF-SEM was fitted using $\lambda_X = 100$ and sparsity parameters (λ_1, λ_2) chosen to minimize the 5-fold equilibrium MAE. The estimated latent-feedback operator was extremely weak: $\rho(X\Theta_1) \approx 0.003$, and the amplification ratio was nearly one ($AR \approx 1.002$), indicating that weekly mortality responds almost entirely to direct environmental inputs rather than latent feedback.

The estimated basis matrix X (Table 4) separates respiratory mortality (Factor 1) from the combined pattern of cardiovascular and total mortality (Factor 2).

Table 4 Estimated basis matrix X for LA pollution data ($Q = 2$).

Variable	Factor 1	Factor 2
Respiratory mortality	1.00	0.00
Total mortality	0.00	0.47
Cardiovascular mortality	0.00	0.53

The structural diagram (Figure 2) shows that Factor 1 is primarily activated by climatic variables, whereas Factor 2 is activated by pollutant levels, reflecting distinct exogenous pathways captured by (X, Θ_1, Θ_2) .

These pathways are consistent with epidemiological evidence that pollutants such as CO and SO₂ elevate cardiovascular risk (Brook et al, 2010), and NMF-SEM recovers this distinction in a fully data-driven manner while confirming negligible latent feedback.

Overall, the analysis indicates that NMF-SEM identifies two distinct mortality components and that latent feedback is negligible in this setting.

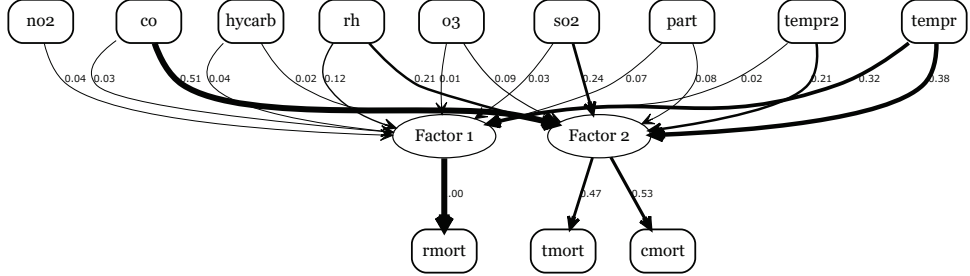


Fig. 2 Path diagram estimated by NMF-SEM ($Q = 2$) for the LA pollution–mortality system. Factor 1 reflects climatic drivers of respiratory mortality, whereas Factor 2 captures pollutant-related variation in cardiovascular and total mortality.

5.3 Mississippi health-risk analysis

County-level data from the 2025 County Health Rankings (CHR) ([University of Wisconsin Population Health Institute, 2025](#)) were used. Eleven social determinants served as exogenous variables (poverty, income, smoking, inactivity, obesity, education, sleep deprivation, PM_{2.5}, housing problems, social association, and teen births), and eleven health outcomes—including early mortality, diabetes, physical and mental distress, infant outcomes, injury and homicide deaths, overdose, suicide, and firearm deaths—were treated as endogenous variables. All variables were rescaled to [0, 1], with protective indicators multiplied by -1 to ensure that larger values represent higher risk.

Cross-validation selected a latent dimension of $Q = 3$. The estimated feedback operator indicated modest latent feedback: $\rho(X\Theta_1) \approx 0.441$ and $AR \approx 1.029$, implying that cumulative effects slightly exceed direct effects.

The estimated basis matrix X (Table 5) yields three interpretable latent components. Factor 1 loads on early mortality, diabetes, physical distress, and infant-related outcomes; Factor 2 loads on mental distress, injury deaths, homicide, and infant mortality; Factor 3 isolates suicide and drug overdose.

Table 5 Estimated basis matrix X for the Mississippi data ($Q = 3$).

Outcome	Factor 1	Factor 2	Factor 3
early_death	0.22	0.00	0.00
diabetes	0.21	0.00	0.00
bad_phys	0.00	0.28	0.00
suicide	0.00	0.00	0.69
bad_ment	0.00	0.31	0.00
low_birth	0.21	0.00	0.00
infant_mort	0.04	0.18	0.00
injury_death	0.00	0.23	0.00
homicide	0.16	0.00	0.00
drug_overdose	0.00	0.00	0.31
firearm_death	0.16	0.00	0.00

The exogenous pathways Θ_2 (Table 6) indicate that Factor 1 is associated with poverty, low income, inactivity, and housing problems; Factor 2 with income, smoking, and housing; Factor 3 with social association and PM_{2.5}.

Table 6 Estimated structural coefficients Θ_2 (drivers \rightarrow latent factors).

Driver	F1	F2	F3
child_pov	1.94	0.01	0.00
income	0.16	2.03	0.08
smoking	0.00	0.54	0.05
inactivity	1.21	0.00	0.00
obesity	0.25	0.05	0.00
hs_grad	0.00	0.06	0.00
sleep	0.12	0.05	0.00
pm25	0.00	0.00	0.11
housing	0.44	0.48	0.00
social_assoc	0.00	0.36	0.44
teen_birth	0.00	0.17	0.00

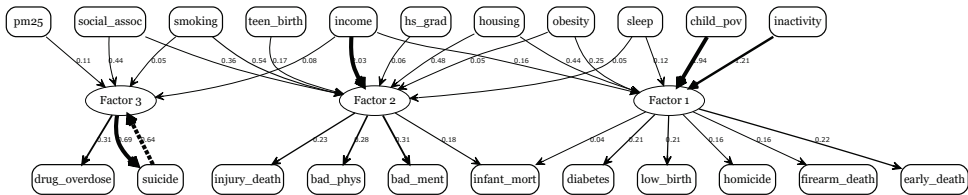


Fig. 3 Path diagram estimated by NMF-SEM ($Q = 3$) for Mississippi counties. The diagram reflects the structural relations encoded by (X, Θ_1, Θ_2) .

These latent pathways align with recent research emphasizing that “deaths of despair”—including suicide and drug overdose—are driven primarily by social isolation and weakened community ties rather than by material deprivation alone (Case and Deaton, 2020). NMF-SEM isolates this mechanism as a distinct latent component and quantifies how social association and environmental exposures propagate to these outcomes through the equilibrium mapping.

The model exhibits high structural fidelity ($SC_{map} = 0.935$, $SC_{cov} = 0.989$) and moderate prediction error ($MAE = 0.116$). These results indicate that NMF-SEM provides a coherent non-negative decomposition of county-level health outcomes and identifies distinct exogenous pathways for each latent component, while latent feedback remains limited given the small sample size ($N = 36$).

6 Discussion and conclusion

This paper introduced NMF-SEM, a non-negative structural equation framework that embeds NMF within a simultaneous equation system. By parameterizing the coefficient

matrix as $B = \Theta_1 Y_1 + \Theta_2 Y_2$, the method links latent components to both endogenous and exogenous variables and yields a well-defined equilibrium representation. The resulting Leontief-type operator provides a principled way to decompose direct and cumulative effects in non-negative systems.

NMF-SEM makes four main contributions. First, it provides a cycle-permissive non-negative structural system in latent space. Second, it yields an equilibrium mapping whose Neumann expansion separates direct and higher-order feedback effects. Third, it offers a regularized estimation strategy that combines orthogonality and sparsity. Fourth, it introduces structural evaluation metrics—distinct from reconstruction error—that quantify input–output fidelity, second-moment structure, and feedback strength.

Empirical applications showed that NMF-SEM distinguishes systems dominated by direct effects from those exhibiting moderate or weak latent feedback. The Holzinger–Swineford data displayed moderate amplification, the Los Angeles pollution–mortality system was effectively feed-forward, and the Mississippi health-risk data exhibited weak latent feedback. These results indicate that NMF-SEM provides a coherent non-negative decomposition of county-level health outcomes and identifies distinct exogenous pathways for each latent component, while latent feedback remains limited given the small sample size ($N = 36$). Because the Mississippi dataset is small ($N = 36$), all structural conclusions are based on equilibrium metrics and bootstrap percentiles rather than on individual parameter estimates.

Simulation experiments further demonstrated that NMF-SEM reliably recovers input–output structure under noise and that the feedback metrics behave consistently with the true data-generating process. Bootstrap percentile intervals for $\rho(X\Theta_1)$ and AR (obtained as described in Section 4.3) were tightly centered around their point estimates, confirming that the inferred levels of latent feedback are stable across datasets.

Consistent with the numerical experiments, all three empirical applications displayed high SC_{map} , indicating that the equilibrium operator M_{model} is stably recovered even though (Θ_1, Θ_2) themselves are not identifiable. The equilibrium prediction errors (MAE) were moderate but consistent with the scale of the normalized data, and SC_{cov} was high across datasets, showing that the similarity structure of Y_1 is well reproduced in real data as well as in the controlled simulations.

Several limitations warrant mention. First, (Θ_1, Θ_2) are not uniquely identifiable; emphasis should therefore be placed on equilibrium behavior rather than on the individual parameter values. Second, interpretable solutions often require strong regularization. Third, the current formulation assumes a static equilibrium and does not model temporal evolution.

Future work includes developing dynamic extensions that incorporate time-series structure, uncertainty quantification for equilibrium effects, and hybrid models that integrate graphical or network constraints. Applications to large-scale health, environmental, and economic systems are also promising, particularly in settings where intermediate flows are unobserved.

Software availability. All methods described in this paper, including estimation procedures, equilibrium metrics, and visualization tools, are implemented in the `nmfkc`

package (Satoh, 2025c). The package is publicly available at <https://ksatohds.github.io/nmfkc/> and enables full replication of the analyses reported in this study.

In summary, NMF-SEM provides a unified non-negative framework for capturing both direct and cumulative effects in latent structural systems, offering an interpretable tool for analyzing feedback and propagation mechanisms across diverse domains.

References

Boutsidis C, Galloopoulos E (2008) Svd based initialization: A head start for nonnegative matrix factorization. *Pattern recognition* 41(4):1350–1362

Brook RD, Rajagopalan S, Pope III CA, et al (2010) Particulate matter air pollution and cardiovascular disease: an update to the scientific statement from the american heart association. *Circulation* 121(21):2331–2378

Case A, Deaton A (2020) Deaths of Despair and the Future of Capitalism. Princeton University Press, URL <http://www.jstor.org/stable/j.ctvpr7rb2>

Cichocki A, Zdunek R, Phan A, et al (2009) Nonnegative Matrix and Tensor Factorizations: Applications to Exploratory Multi-way Data Analysis and Blind Source Separation. Wiley

Galeano A, Santos S, Jimenez R, et al (2024) Constraining non-negative matrix factorization to improve signature learning. URL <https://openreview.net/forum?id=AcGUW5655J>

Galeano D, Paccanaro A (2022) Machine learning prediction of side effects for drugs in clinical trials. *Cell reports methods* 2(12)

Gillis N (2014) The why and how of nonnegative matrix factorization. *Regularization, optimization, kernels, and support vector machines* 12(257):257–291

Holzinger KJ, Swineford F (1939) A study in factor analysis: The stability of a bi-factor solution. *Supplementary educational monographs*

Jöreskog KG (1969) A general approach to confirmatory maximum likelihood factor analysis. *Psychometrika* 34(2):183–202

Lee D, Seung HS (2000) Algorithms for non-negative matrix factorization. In: Leen T, Dietterich T, Tresp V (eds) *Advances in Neural Information Processing Systems*, vol 13. MIT Press, URL https://proceedings.neurips.cc/paper_files/paper/2000/file/f9d1152547c0bde01830b7e8bd60024c-Paper.pdf

Lee DD, Seung HS (1999) Learning the parts of objects by non-negative matrix factorization. *Nature* 401(6755):788–791

Leontief WW (1936) Quantitative input and output relations in the economic systems of the united states. *The Review of Economic Statistics* pp 105–125

Lodhia A, Hütter JC, Uhler C, et al (2023) Positivity in linear gaussian structural equation models. arXiv preprint arXiv:230519884

Satoh K (2024) Applying non-negative matrix factorization with covariates to the longitudinal data as growth curve model. URL <https://arxiv.org/abs/2403.05359>, [2403.05359](https://arxiv.org/abs/2403.05359)

Satoh K (2025a) Applying non-negative matrix factorization with covariates to label matrix for classification. URL <https://arxiv.org/abs/2510.10375>, [2510.10375](https://arxiv.org/abs/2510.10375)

Satoh K (2025b) Applying non-negative matrix factorization with covariates to multivariate time series data as a vector autoregression model. *Japanese Journal of Statistics and Data Science* <https://doi.org/10.1007/s42081-025-00314-0>, URL <https://doi.org/10.1007/s42081-025-00314-0>

Satoh K (2025c) nmfkc: Non-Negative Matrix Factorization with Covariates and Structural Extensions. URL <https://ksatohds.github.io/nmfkc/>, r package version 0.5.8

Shumway RH, Stoffer DS (2006) Time series analysis and its applications: with R examples. Springer

University of Wisconsin Population Health Institute (2025) County Health Rankings & Roadmaps 2025 Analytic Dataset (Supplemental Data Release). URL <https://www.countyhealthrankings.org/health-data/methodology-and-sources/data-documentation>, dataset accessed via <https://www.countyhealthrankings.org>. Includes Supplemental Data Release dated November 4, 2025

Zhang YQ, Tian GL, Tang NS (2016) Latent variable selection in structural equation models. *Journal of Multivariate Analysis* 152:190–205

Zhou R, Ying J, Palomar DP (2022) Covariance matrix estimation under low-rank factor model with nonnegative correlations. *IEEE Transactions on Signal Processing* 70:4020–4030